Available online at www.sciencedirect.com
SCIENCE DIRECT
Optics Communications 261 (2006) 23–28
OPTICS COMMUNICATIONS
www.elsevier.com/locate/optcom

Development and investigation of an optical tilt sensor

Z.W. Zhong [a,*], L.P. Zhao [b], H.H. Lin [a]

[a] School of Mechanical and Aerospace Engineering, Nanyang Technological University, 50 Nanyang Avenue, Singapore 639798, Republic of Singapore
[b] Singapore Institute of Manufacturing Technology, 71 Nanyang Drive, Singapore 638075, Republic of Singapore

Received 3 August 2005; received in revised form 14 November 2005; accepted 20 November 2005

Abstract

An optical tilt sensor was developed and its performance was investigated. The tilt sensor set-up consisted of a laser light source, lenses and an image sensor. A precision reference tilt sensor was also installed on the same stage, and the measurement results of tilt angles using the optical and reference tilt sensors were correlated. The correlation coefficient (R-value) obtained under ideal conditions was 0.99454, indicating that the optical tilt sensor could produce as accurate measurements as the precision reference tilt sensor. The R-value decreased to 0.97714 and 0.93209 when the image sensor was shifted backwards and forwards from the focal plane by 1 mm, respectively. The R-value decreased to 0.96840 when the tilt sensor was performed with the room light turned on. There were not significant differences in the measurement results obtained with air conditioners turned on and off, indicating that the optical tilt sensor was robust and was not sensitive to the surrounding air turbulence. These findings are useful for the final design of the optical tilt sensor.

PACS: 07.07.Df; 42.15.Dp; 42.62.Eh

Keywords: Optical sensor; Tilt sensor; Correlation coefficient

1. Introduction

Tilt sensors [1] create an artificial horizon and measure the angular tilt with respect to that horizon. They are used in aircraft flight controls, cameras, automobile systems and special switches.

Electrolytic tilt sensors [2] are inexpensive and can produce accurate pitch and roll measurements in a variety of applications [1]. They exhibit excellent repeatability and 8 stability when they are operating at low frequencies. However, their sensitivity to both external and internal influences makes them complex devices that have to be understood before installation and operation. Electrolytic sensors come in a variety of packages with varying tilt resolution and ranges [3]. Applications include antenna positioning, automotive testing and tilt monitoring [2].

Capacitive tilt sensors are designed to take non-contact measurements of inclinations and tilt [1]. They have many advantages [4]: low power usage and cost, and good stability, speed and resolution. They can be optically transparent, and are easy to be integrated into integrated circuits or onto printed-circuit boards. Capacitive sensors [5,6] can directly sense motion, electric field and chemical composition, and indirectly sense acceleration, pressure, fluid composition and fluid level. However, they are affected by temperature and humidity, and are sensitive to noise [4].

Liquid tilt sensors are inexpensive, but they are fragile and have ''slosh'' problems [1]. A mercury type tilt sensor consists of a small glass or metal can, inside of which are two electrodes and a minute drop of mercury. Its operation is based on the tilted position of the sensor [7].

A high-precision pendulum tilt sensor was used in this study for comparison. This sensor [8] is basically a pendulum used in conjunction with an electronic detecting system to precisely sense the attitude of the pendulum with respect to its housing. An inductive bridge circuit is utilized to

* Corresponding author. Tel.: +65 6790 5588; fax: +65 6791 1859.
E-mail address: mzwzhong@ntu.edu.sg (Z.W. Zhong).

0030-4018/$ - see front matter © 2005 Elsevier B.V. All rights reserved.
doi:10.1016/j.optcom.2005.11.044

obtain an electrical signal, which is then amplified, to operate an analogue meter and a liquid crystal display.

Wave-front sensing is an essential part of adaptive optics, vision optics, and optical and silicon manufacturing [9–11]. A wave-front sensor [12] can be used either to measure wave fronts, or, in combination with a deformable mirror, to perform wave-front correction. There are many types of wave-front sensors such as the Hartmann wave-front sensor, the curvature wave-front sensor, the phase diversity wave-front sensor and the shearing interferometer [12–15].

One method to test a lens or mirror employs an opaque mask with holes placed behind the optical element under test. Each of the holes acts as an aperture, and because the light passing through the lens is converging, the image produced is an array of spots. With proper calibration, the position of the spots is a direct indication of the local wave-front tilt at each hole and hence a description of the lens quality. This test is called the Hartmann test [14].

Variations of this technique especially for real-time wave-front measurements are used in adaptive optics wave-front sensors. Shack expanded the concept, placed lenses in the holes, which increased the light gathering efficiency of the mask and reduced the disturbing diffraction effects of the holes with the spots focused [16,17]. This sensor was called the Shack–Hartmann wave-front (SHWF) sensor.

The SHWF sensor uses the fact that light travels in a straight line to measure the wave front of light. A lenslet array breaks an incoming beam into multiple focal spots falling on an optical detector. By sensing the position of the focal spots, the propagation vector of the sampled light can be calculated for each lenslet and the wave front can be reconstructed from the vectors [18]. Local slopes cause the beams or the foci to move off their nominal positions by an amount proportional to the distance between the holes or the lenslets and the detector. An image of the whole-distorted pattern of spots is analyzed to find the location of every spot. Calculation is performed on a sub-region around the expected location of each spot to find its centroid. The locations of the reference spots are subtracted to compare the wave front to certain reference wave front. The difference is broken into the x and y components of the gradient of the wave front to be further analyzed [10,17,19–26].

SHWF sensors are finding increasingly more uses as multipurpose optical-laboratory tools [27,28]. Their popularity is correlated with three main factors [18,25,27,29]: inherent conceptual simplicity, their specific features and the availability of the key components required for gathering data and processing them at a reasonable speed.

In this study, an optical tilt sensor was built and tested. The measurement results were compared to those obtained using a precision reference tilt sensor. Various experiments were conducted to investigate the performance of the optical tilt sensor under various conditions such as air turbulence and surrounding light.

2. Experimental set-up

Fig. 1 displays the schematic diagram of the experimental set-up and Table 1 shows the functions of the components used in the set-up. The main components required for the experimental set-up are a He–Ne laser source, lenses and an image sensor.

An objective lens focused laser light into a ϕ10-μm pinhole, which was placed at the focal plane of the objective lens. A collimating lens with a 600-mm focal length was placed at a distance of 600 mm from the pinhole. A plane wave front was produced from the collimating lens. A focusing lens with a 3-mm focal length was placed on a rotating frame, which could be adjusted so that the focusing lens could be tilted at a certain angle.

The laser light passed through the focusing lens and generated a light spot on the image sensor, which was positioned in the focal plane of the lens and captured the image of the light spot. The image was then input into an image-processing unit to calculate the centroid shift of the light spot and the tilt angle.

Image processing plays an important role in many applications [30,31]. Fig. 2 shows the flowchart of the image-processing unit. To calculate the centroid shift, the images captured by the image sensor were processed using a centroid-finding program. A reference image was the image of the light spot at the start of a measurement experiment, while a measured image was the image of the light spot after a tilt angle was introduced to the system.

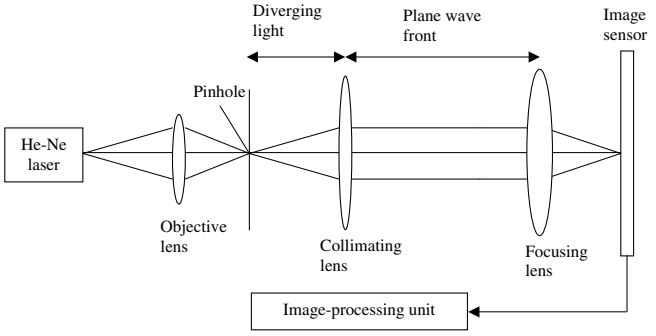

Fig. 1. Schematic diagram of the experimental set-up.

Table 1
Functions of the components used in the experimental set-up

Components	Function
He–Ne laser source (15 mW, 632.8 nm)	Light source
Objective lens	To focus light into the pinhole
Pinhole of ϕ10 μm	To filter light
Collimating lens with a 600-mm focal length	To produce plane wave front
Focusing lens with a 3-mm focal length	To generate a light spot on the image sensor
Image sensor	To capture the image of the light spot
Image-processing unit	To calculate the centroid shift and tilt angle

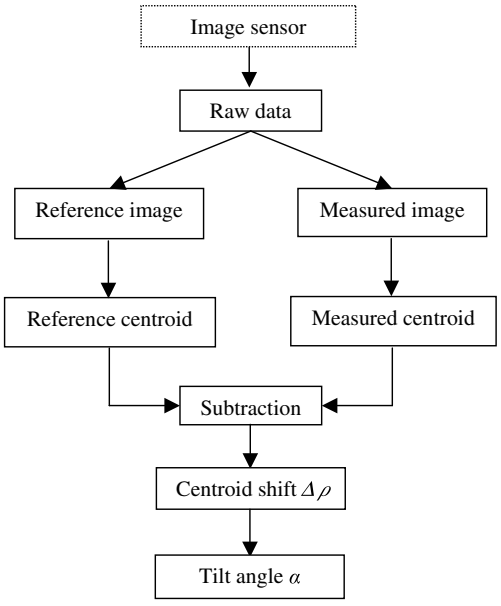

Fig. 2. Flowchart of the image-processing unit.

The centroid-finding program calculated ρ_{ref} (the centroid of the reference image) and ρ (the centroid of the measured image). The difference of the centroids was the centroid shift $\Delta\rho$, as shown below:

$$\Delta\rho = \rho - \rho_{ref} \quad (1)$$

Because the focal length of the focusing lens f is known, the tilt angle α can be expressed as:

$$\tan\alpha = \frac{\Delta\rho}{f} \quad (2)$$

Because the tilt sensor can only measure small angles, Eq. (2) can be expressed as:

$$\alpha = \frac{\Delta\rho}{f} \quad (3)$$

According to Eq. (3), the tilt angle α is directly proportional to the centroid shift $\Delta\rho$ because f is a constant. Therefore, the centroid shift $\Delta\rho$ obtained from the optical tilt sensor can be directly compared to the corresponding tilt angle value obtained from a reference tilt sensor.

A precision pendulum tilt sensor was utilized as the reference tilt sensor. Its two level-units were also placed on the rotating frame together with the focusing lens. This sensor has resolution of 0.1″, accuracy of ±(0.2 + 2% of displayed value) arc sec, and a range of ±600″ [32]. The measurement results using the reference and optical tilt sensors were compared.

3. Measurements of tilt angles

Factors that might affect the performance of the optical tilt sensor were investigated. They included atmospheric turbulence, the distance between the focusing lens and the image sensor, and the surrounding light. The investigation of the key factors is important for the final design of the optical tilt sensor.

3.1. Atmospheric turbulence

Naturally occurring small variations in temperature (<1 °C) cause small changes in wind velocity, the atmospheric density and the index of refraction. These changes can accumulate, and the cumulative changes can cause significant inhomogenities in the index profile of the atmosphere. The wave front of a beam will change in the course of propagation. This can lead to beam wandering, intensity fluctuations, and beam spreading. The small changes in the index of refraction act like small lenses in the atmosphere. They focus and redirect waves and cause intensity variations [14,22].

The effects of the atmospheric turbulence on the accuracy of the optical tilt sensor were investigated in this study. Experiments were conducted with the room light turned off and with air conditioners turned on or off. For every tilt angle measured, three images of the light spot were captured at 1-min intervals. The centroid measurements of the light spot were performed and averaged, and the centroid shifts were calculated.

Based on the readings of the reference and optical tilt sensors, fitted curves were plotted, as shown in Figs. 3 and 4. The fitted curve equation obtained from the experiments conducted with air conditioners turned on is $y = 559.6 - 438.7x$, and the correlation coefficient (R-value) is −0.99443. The higher the absolute R-value, the better is the linearity of the graph. The fitted curve equation obtained from the experiments conducted with air conditioners turned off is $y = 560.3 - 439.2x$, and the R-value is −0.99454, which is slightly better than −0.99443. The differences are small, indicating that the tilt sensor is robust and is not sensitive to the surrounding air turbulence.

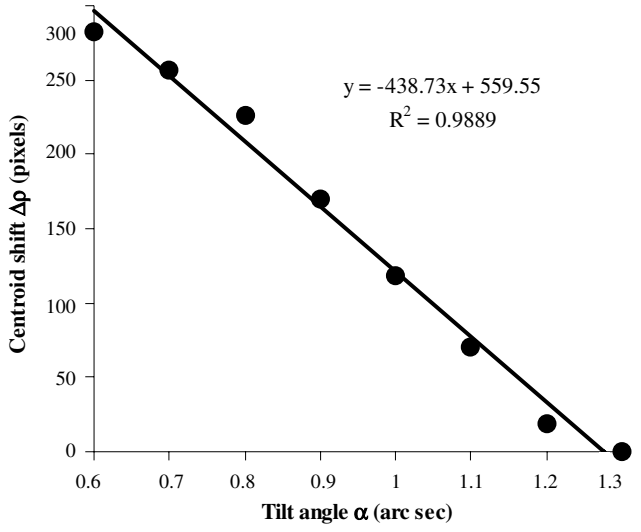

Fig. 3. Correlation of readings from the reference and optical tilt sensors (Experiments were conducted with air conditioners turned on).

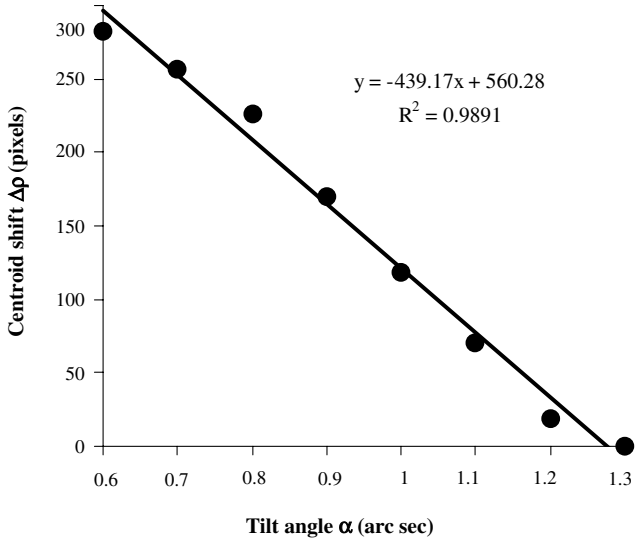

Fig. 4. Correlation of readings from the reference and optical tilt sensors (Experiments were conducted with air conditioners turned off).

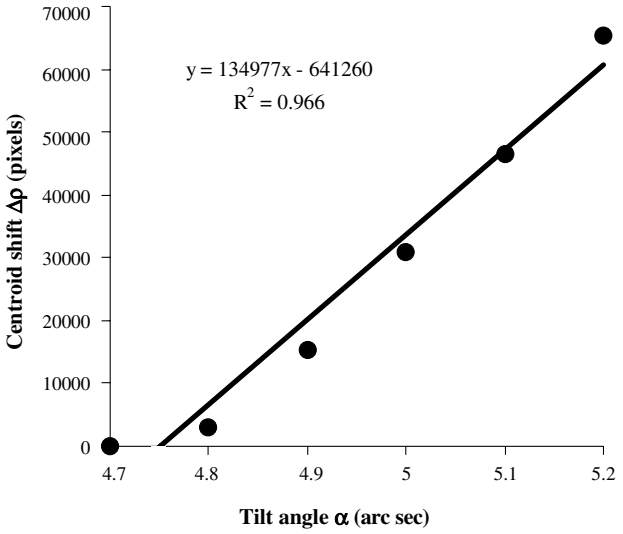

Fig. 6. Optical tilt sensor readings versus reference tilt sensor readings when the image sensor was placed in the focal plane of the focusing lens.

3.2. Distance between the focusing lens and image sensor

Experiments were performed to investigate the effect of the distance between the focusing lens and image sensor on the measurement accuracy of the optical tilt sensor. One experiment was conducted by placing the image sensor in the focal plane of the focusing lens. Two experiments were conducted by shifting the image sensor 1 mm backwards and forwards from the focal plane respectively. These experiments were conducted with room light turned off.

Fig. 5 shows the reference images of the light spots captured by the image sensor that was placed at different distances away from the focal plane. The light spot became bigger when the image sensor was shifted either backwards or forwards by 1 mm from the focal plane.

Fig. 6 shows the optical tilt sensor readings versus the reference tilt sensor readings when the image sensor was placed in the focal plane of the focusing lens. The fitted curve equation was $y = -641{,}260 + 134{,}977x$, and the R-value obtained was 0.98285.

Fig. 7 shows the optical tilt sensor readings versus the reference tilt sensor readings when the image sensor was shifted backwards by 1 mm from the focal plane. The fitted curve equation and the R-value achieved were $y = -461{,}524 + 97{,}370x$ and 0.97714, respectively. The R-value in this case was lower than 0.98285 in Fig. 6.

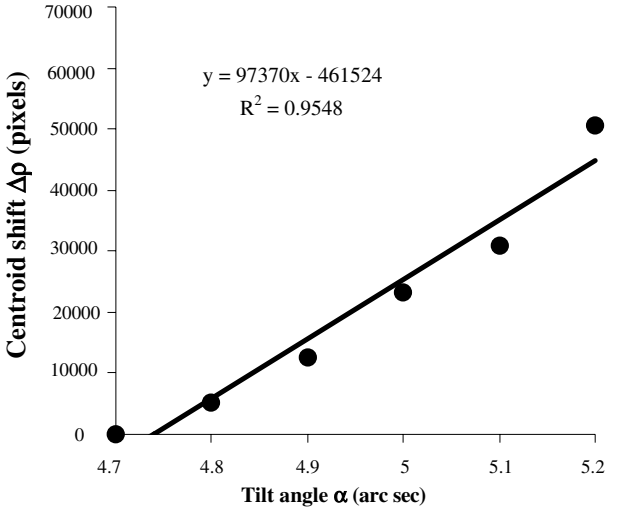

Fig. 7. Optical tilt sensor readings versus reference tilt sensor readings when the image sensor was shifted backwards by 1 mm from the focal plane.

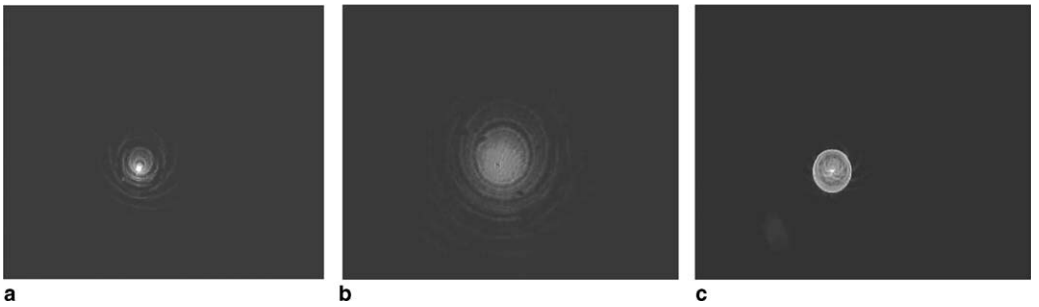

Fig. 5. Reference images of the light spots captured by the image sensor that was placed at different distances away from the focal plane. (a) The image sensor was in the focal plane. (b) The image sensor was shifted backwards by 1 mm. (c) The image sensor was shifted forwards by 1 mm.

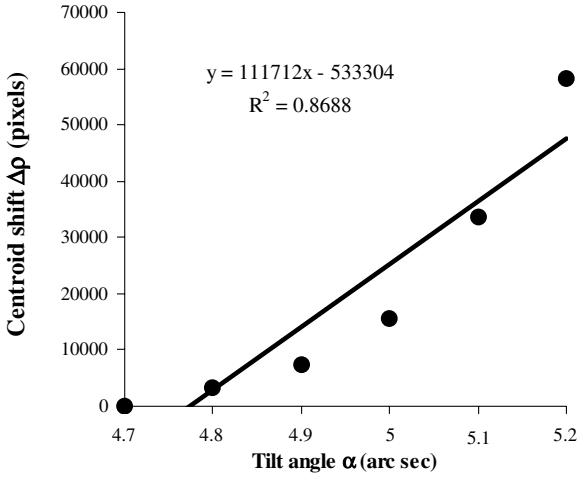

Fig. 8. Optical tilt sensor readings versus reference tilt sensor readings when the image sensor was shifted forwards by 1 mm from the focal plane.

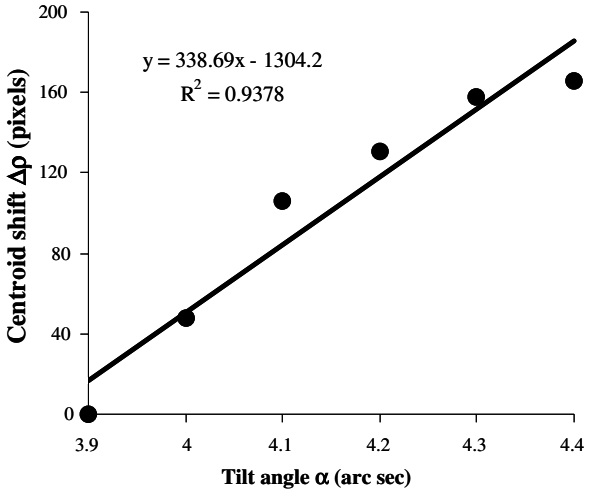

Fig. 9. Optical tilt sensor readings versus reference tilt sensor readings obtained with the room light turned on.

Fig. 8 shows the optical tilt sensor readings versus the reference tilt sensor readings when the image sensor was shifted forwards by 1 mm from the focal plane. The fitted curve equation achieved was $y = -533{,}304 + 111712x$. The R-value was 0.93209 and was also lower than 0.98285 in Fig. 6.

Of these three experiments, the highest R-value was obtained when the image sensor was placed in the focal plane of the focusing lens. When the image sensor was shifted backwards or forwards by 1 mm from the focal plane, the R-value decreased. The distance does affect the overall sensitivity and the accuracy of the measurements. It is important to obtain the correct focal spot (the brightest and smallest light spot) as the reference image at the start of the measurements.

3.3. Surrounding light

Proper surrounding light or lighting is important in many image processing applications [33,34]. In this application, the surrounding light might also affect the accuracy of the readings of the optical tilt sensor, and therefore its effect was investigated. Images were captured with the room light turned on. The optical tilt sensor readings versus the reference tilt sensor readings are shown in Fig. 9. The fitted curve equation was $y = -1304.2 + 338.7x$, and the R-value was 0.96840.

The linearity of the curve in Fig. 9 is not as good as the curves in Figs. 3, 4 and 6 achieved with the room light turned off, and the R-value obtained from the experiment conducted with the room light turned on was lower than those values obtained with the room light turned off. This was because the image sensor captured the laser light spot and the surrounding room light in this case. As a result, the background intensity distribution also contributed to the centroid calculation. Because the background light intensity distribution was not uniform when the focusing lens

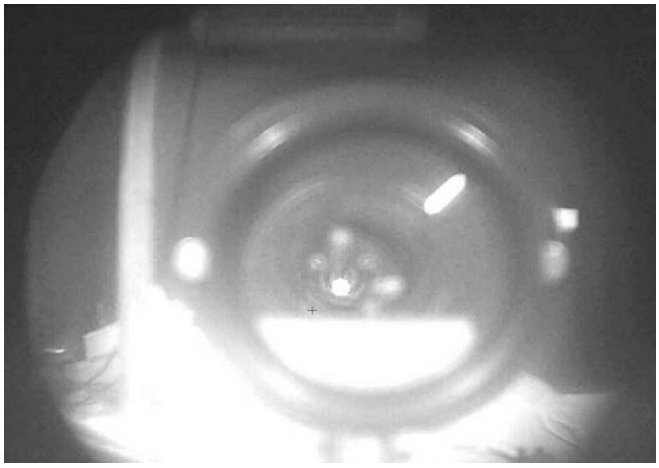

Fig. 10. An image obtained when the room light was turned on.

was tilted as shown in Fig. 10, the centroid of the light spot calculated was not accurate. The cross mark in the picture indicates the centroid position that was inaccurately calculated by the centroid-finding program.

To find the correct centroid position of the light spot, measurements using the optical tilt sensor should be performed with the room light turned off. The final prototype of the optical tilt sensor should have a properly designed casing to shelter out the noise light from the surroundings.

4. Conclusions

An optical tilt sensor set-up was built using a laser light source, optical lenses and an image sensor. A precision reference tilt sensor was also installed on the same stage. The experimental results of the optical and reference tilt sensors were correlated and the R-value achieved under ideal conditions was 0.99454. Experiments were conducted to study the key factors that might affect the performance of the optical tilt sensor. When the image sensor was shifted

backwards and forwards from the focal plane by 1 mm, the *R*-value decreased to 0.97714 and 0.93209, respectively. The *R*-value decreased to 0.96840 when the tilt sensor was performed with the room light turned on. The experiments conducted have proved that the optical tilt sensor is able to produce as accurate measurements as the reference tilt sensor under ideal conditions.

References

[1] Global Specs Inc., About tilt sensors and inclinometers, Available from: <http://sensors-transducers.globalspec.com/LearnMore/Sensors_Transducers_Detectors/Tilt_Sensing/Tilt_Inclinometers>, 2004.

[2] W.B. Powell, D. Pheifer, The electrolytic tilt sensor, Available from: <http://www.sensorsmag.com/articles/0500/120/main.shtml>, 2004.

[3] Spectron Glass and Electronics Inc., Electrolytic tilt sensors, Available from: <http://www.spectronsensors.com>, 2004.

[4] Planet EE Network, Electronic design, Available from: <http://www.elecdesign.com/Articles/Index.cfm?ArticleID=7653&pg=1>, 2004.

[5] The PI-Polytec Group, Capacitive position sensors/controllers, Available from: <http://www.capacitance-sensors.com>, 2004.

[6] L.K. Baxter, Capacitive sensors, Available from: <http://sensors-transducers.globalspec.com/goto /PDFViewer?pdfURL=http%3A%2F%2Fwww%2Ecapsense%2Ecom%2Fcapsense%2Dwp%2Epdf>, 2004.

[7] George Risk Industries, 4561 Mercury tilt sensor, Available from: <http://www.grisk.com/specialty/4561.htm>, 2004.

[8] Taylor Hobson Limited, Talyvel 4 differential system, Available from: <http://esales.taylor-hobson.com/sterling/acatalog/sterling_Instruments_15.html>, 2005.

[9] Z.W. Zhong, S.C. Lim, A. Asundi, Journal of Electronic Packaging 127 (1) (2005) 25.

[10] A. Talmi, E.N. Ribak, Journal of the Optical Society of America A-Optics Image Science and Vision 21 (4) (2004) 632.

[11] R. Ragazzoni, S.R. Restaino, Optics Communications 137 (1–3) (1997) 6.

[12] J.M. Geary, Introduction to Wavefront Sensors, SPIE Press, Bellingham, Wash., 1995.

[13] O. Guyon, The UH AO system. March, Available from: <http://www.ifa.hawaii.edu/ao/system/curv.html>, 2004.

[14] R.K. Tyson, Principles of Adaptive Optics, Academic Press, Boston, 1991.

[15] R. Ragazzoni, E. Diolaiti, E. Vernet, Optics Communications 208 (1–3) (2002) 51.

[16] B.C. Platt, R. Shack, Journal of Refractive Surgery 17 (2001) 573.

[17] M. Mansurripur, Classical Optics and its Applications, Press Syndicate of the University of Cambridge, Cambridge, UK, 2002.

[18] R.R. Rammage, D.R. Neal, R.J. Copland, Proceedings of SPIE 4779 (2002) 161.

[19] R.K. Tyson, B.W. Frazier, Field Guide to Adaptive Optics, SPIE Press, Bellingham, Washington, 2004.

[20] Y. Zhang, D. Yang, X. Cui, Applied Optics 43 (4) (2004) 729.

[21] S. Oliver, V. Laude, J.-P. Huignard, Applied Optics 39 (22) (2000) 3838.

[22] M.L. Plett, P.R. Barbier, D.W. Rush, P. Polak-Dingels, B.M. Levine, Available from: <http://www.markplett.com/pub/spie.pdf>, 2004.

[23] R.B. Own, A.A. Zozulya, Applied Optics 41 (28) (2002) 5891.

[24] H. Hamam, Optics Communication 173 (2000) 23.

[25] L. Seifert, J. Liesener, H.J. Tiziani, Optics Communications 216 (2003) 313.

[26] J.D. Mansell, E.K. Gustafson, Applied Optics 40 (7) (2001) 1074.

[27] J. Ares, T. Mancebo, S. Bara, Applied Optics 39 (10) (2000) 1511.

[28] L. Seifert, J. Liesener, H.J. Tiziani, Optics Communications 216 (4–6) (2003) 313.

[29] J.A. Koch, R.W. Presta, R.A. Sacks, R.A. Zacharias, E.S. Bliss, M.J. Dailey, M. Feldman, A.A. Grey, F.R. Holdener, J.T. Salmon, L.G. Seppala, J.S. Toeppen, L. Van Atta, B.M. Van Wonterghem, W.T. Whistler, S.E. Winters, B.W. Woods, Applied Optics 39 (25) (2000) 4540.

[30] N.G. Shankar, Z.W. Zhong, N. Ravi, Defects and Diffusion Forum 230–232 (2004) 135.

[31] N.G. Shankar, Z.W. Zhong, Microelectronic Engineering 77 (3–4) (2005) 337.

[32] The European Synchrotron Rradiation Facility, Electronic level. Available from: <http://www.esrf.fr/UsersAndScience/Experiments/TBS/MechanicsService/PELab/ElectronicLevel>, 2005.

[33] Z.W. Zhong, Y. Jiang, Materials and Manufacturing Processes 19 (3) (2004) 439.

[34] Z.W. Zhong, Y. Jiang, Microelectronics International 21 (2) (2004) 41.